

# Genome-wide survey by ChIP-seq reveals YY1 regulation of lincRNAs in skeletal myogenesis

Leina Lu<sup>1,3</sup>, Kun Sun<sup>1,3</sup>, Xiaona Chen<sup>2</sup>,  
Yu Zhao<sup>2</sup>, Lijun Wang<sup>2</sup>, Liang Zhou<sup>2</sup>,  
Hao Sun<sup>1,\*</sup> and Huating Wang<sup>2,\*</sup>

<sup>1</sup>Department of Chemical Pathology, Li Ka Shing Institute of Health Sciences, Prince of Wales Hospital, The Chinese University of Hong Kong, Hong Kong, China and <sup>2</sup>Department of Obstetrics and Gynaecology, Li Ka Shing Institute of Health Sciences, Prince of Wales Hospital, The Chinese University of Hong Kong, Hong Kong, China

**Skeletal muscle differentiation is orchestrated by a network of transcription factors, epigenetic regulators, and non-coding RNAs. The transcription factor Yin Yang 1 (YY1) silences multiple target genes in myoblasts (MBs) by recruiting Ezh2 (Enhancer of Zeste Homologue2). To elucidate genome-wide YY1 binding in MBs, we performed chromatin immunoprecipitation (ChIP)-seq and found 1820 specific binding sites in MBs with a large portion residing in intergenic regions. Detailed analysis demonstrated that YY1 acts as an activator for many loci in addition to its known repressor function. No significant co-occupancy was found between YY1 and Ezh2, suggesting an additional Ezh2-independent function for YY1 in MBs. Further analysis of intergenic binding sites showed that YY1 potentially regulates dozens of large intergenic non-coding RNAs (lincRNAs), whose function in myogenesis is under-explored. We characterized a novel muscle-associated lincRNA (Yam-1) that is positively regulated by YY1. Yam-1 is downregulated upon differentiation and acts as an inhibitor of myogenesis. We demonstrated that Yam-1 functions through *in cis* regulation of miR-715, which in turn targets Wnt7b. Our findings not only provide the first genome-wide picture of YY1 association in muscle cells, but also uncover the functional role of lincRNA Yam-1.**

*The EMBO Journal* (2013) 32, 2575–2588. doi:10.1038/emboj.2013.182; Published online 13 August 2013

**Subject Categories:** chromatin & transcription; RNA; differentiation & death

**Keywords:** ChIP-seq; lincRNA; myogenesis; PRC2; YY1; Yam-1

## Introduction

Normal skeletal muscle growth as well as the regeneration of damaged muscle fibres in post-embryonic life are attributed

\*Corresponding authors. H Sun, Department of Chemical Pathology, Li Ka Shing Institute of Health Sciences, Prince of Wales Hospital, The Chinese University of Hong Kong, Hong Kong, NT, China. Tel.: +852 3763 6048; Fax: +852 2636 5090;

E-mail: haosun@cuhk.edu.hk or H Wang, Department of Obstetrics and Gynaecology, The Chinese University of Hong Kong, Room 507A, Li Ka Shing Institute of Health Sciences, Prince of Wales Hospital, The Chinese University of Hong Kong, Hong Kong, NT, China. Tel.: +852 3763 6047; Fax: +852 2632 0008; E-mail: huating.wang@cuhk.edu.hk

<sup>3</sup>These authors contributed equally to this work.

Received: 15 November 2012; accepted: 9 July 2013; published online: 13 August 2013

to satellite cells (muscle stem cells), which are characterized by the expression of paired-box transcription factor 7 (Pax7) and when activated, become immature muscle cells or myoblasts (MBs) that will proliferate and differentiate (Buckingham, 2006). The molecular characterization of the late stages of myogenesis has been studied in-depth in a mouse C2C12 MB cell line. The formation of mature muscle proceeds with the exit of MBs from the cell cycle, the expression of muscle-specific genes, and the suppression of genes that are specific to other cell lineages and tissues (Buckingham, 2006). A major portion of our understanding of myogenic differentiation is focused at the level of transcription, orchestrated by a complex network of muscle-specific transcription factors (TFs), including MyoD family (MyoD, Myf5, Myogenin, and MRF4), and MEF2 family (MEF2A-D). These factors coordinate with other transcriptional regulators in a stage-specific manner to activate the differentiation program by inducing or repressing gene transcriptions (Sabourin and Rudnicki, 2000). In addition to TFs, epigenetic regulators exert an important layer of transcriptional control (Perdiguero *et al*, 2009). The interplays between TFs and these regulators on muscle loci constitute an essential part of the regulatory networks.

Yin Yang 1 (YY1) is a multifunctional TF, which regulates various processes of development and differentiation (Gordon *et al*, 2006). It is highly expressed in proliferating MBs and gradually downregulated when differentiation starts, playing essential roles in the transcriptional regulation of myogenesis (Wang *et al*, 2007). Most of the previous work from our group and others identified YY1 as an epigenetic repressor of multiple muscle genes (Caretta *et al*, 2004; Wang *et al*, 2007, 2008) although YY1 is well known to play dual roles in either repressing or activating the transcription depending on the cofactors that it recruits (Deng *et al*, 2010). In proliferating MBs, activated by NF- $\kappa$ B signalling, YY1 functions to repress muscle loci by recruiting histone methyltransferase Ezh2 (Enhancer of Zeste Homologue2) containing Polycomb repressive complex 2 (PRC2) to target loci, which causes trimethylation of lysine 27 of histone 3 (H3K27me3) to silence transcription. When myogenesis ensues, YY1 and the repressive complex are replaced by MyoD/PCAF/SRF complex that activates gene expression. Identified YY1 repressive targets include not only muscle structural genes, such as Myosin heavy chain (MyHC), Troponin, and alpha skeletal actin ( $\alpha$ -Actin), but also several muscle relevant miRNAs, miR-29, miR-1, miR-133, and miR-206 (Wang *et al*, 2008; Lu *et al*, 2012). The interplays between YY1 and muscle loci thus constitute essential components of myogenic network. Recently, we also showed that YY1 regulates a large number of additional miRNAs uncovered by genome-wide computational prediction (Lu *et al*, 2012). Deregulation of the YY1-miRNA circuitries could lead to aberrant myogenic differentiation, which contributes to pathogenesis of Rhabdomyosarcoma and Duchenne muscular dystrophy (Wang *et al*, 2008, 2012; Zhou *et al*, 2012a). Moreover, YY1/PRC2 was

found to modulate muscle stem cell proliferation through regulating Pax7 promoter (Palacios *et al*, 2010) and to regulate insulin/IGF pathway in myotubes (MTs) (Blattler *et al*, 2012). These studies highlight the importance of YY1 in muscle development and the need to determine the full range of loci bound and regulated by YY1 in muscle cells at a genome-wide level.

Ezh2/PRC2, the core component of YY1-mediated transcriptional repression, is known to play key roles in differentiation and development, but its recruitment remains enigmatic. Despite several reports including ours suggested YY1 as a potential recruiting factor for Polycomb activities in mammalian cells, recent studies from embryonic stem (ES) cells did not reveal evident co-occupancy of YY1 and PRC2 genome-wide (Mendenhall *et al*, 2010; Vella *et al*, 2012), pointing to YY1 having PcG-independent functions. It is thus imperative to clarify YY1/PRC2 interplay globally in muscle cells.

Although miRNAs represent a novel family of gene regulators, other classes of non-coding RNAs, particularly long non-coding RNAs (lincRNAs), are emerging as critical regulators of various biological processes. Originally identified by Guttman *et al* (2009) from four mouse cell types using chromatin state maps, large intergenic non-coding RNAs (lincRNAs) are discrete transcriptional unit intervening known protein-coding loci. Approximately 1600 lincRNAs were identified from four types of mouse cells. These transcripts are marked by trimethylation of lysine4 of histone H3 (H3K4me3) at their promoter and trimethylation of lysine36 of histone H3 (H3K36me3) along the length of the transcribed region. This distinctive 'K4-K36 domain' is typical characteristic of transcripts from RNA polymerase II (Pol II). Emerging evidence support the existence of lincRNAs in various biological systems (Guttman *et al*, 2009, 2010, 2011; Khalil *et al*, 2009; Huarte *et al*, 2010; Cabili *et al*, 2011; Paralkar and Weiss, 2011; Prensner *et al*, 2011; Ulitsky *et al*, 2011; Yang *et al*, 2011; Young *et al*, 2012). For example, >8000 human lincRNAs were defined across 24 tissues and cell types (Cabili *et al*, 2011). Very recently, 1119 lincRNA loci were reported in *Drosophila melanogaster* genome (Young *et al*, 2012). Various functions and molecular mechanisms for lincRNAs were suggested, including the regulation of epigenetic marks and gene expression (Khalil *et al*, 2009; Gupta *et al*, 2010; Huarte *et al*, 2010; Tsai *et al*, 2010; Prensner *et al*, 2011), controlling mouse ES cell pluripotency and differentiation (Guttman *et al*, 2011), and modulating reprogramming of human-induced pluripotent stem cells (Loewer *et al*, 2010). However, their involvement in skeletal muscle development remains largely unexplored. It is thus imperative to answer questions like: Are lincRNAs existent in muscle cells? Do they have any impact on myogenic differentiation? Are they components of the TF-mediated transcriptional networks?

In this study, we performed a genome-wide search for YY1-regulated loci by combining high-throughput chromatin immunoprecipitation (ChIP)-sequencing data and expression profiling data from RNA sequencing. Surprisingly, we found that in addition to previous known function as a repressor of genes, YY1 also activates many genes. No significant YY1 and Ezh2 co-occupancy was discovered as originally thought, suggesting PcG-independent function of YY1. Most strikingly, we found a large portion of YY1-binding peaks reside in intergenic

regions, which associate with 63 potential novel lincRNAs named *Yam* (YY1-associated muscle lincRNAs). The expression of one of these lincRNAs, *Yam-1*, was found to be positively regulated by YY1. Further functional studies demonstrated that *Yam-1* acts as an anti-myogenic factor possibly by regulating miR-715, which in turn targets Wnt7b to repress myogenesis. Our studies thus for the first time provide a genome-wide view of YY1 binding in skeletal muscle cells and a novel regulatory axis involving TF, lincRNA, and miRNA.

## Results

### Genome-wide mapping of YY1 binding in C2C12 by ChIP-seq

To gain global insights into the role of YY1 in skeletal myogenesis, we generated high-resolution genome-wide maps of YY1 occupancy in C2C12. Chromatins from proliferating C2C12 MBs or MTs differentiated for 5 days under low mitogen condition were collected for ChIP assay using a YY1 antibody SC-1703 from Santa Cruz. Precipitated DNA fragments, ranging from 100 to 300 nucleotides (nt), were subjected to high-throughput sequencing on an Illumina HiSeq 2000 platform (Supplementary Table S1). A total of 1820 YY1-binding sites were identified with high confidence in MBs. An independent biological replicate yielded a very consistent result with 1097 peaks overlapping between the two replicates (Figure 1A) and a high reproducibility as measured by Irreproducibility Discovery Rate (IDR) analysis (Li *et al*, 2011; Landt *et al*, 2012) (Supplementary Figure S1A and F). To ensure the quality of the data, we used a second antibody against YY1, AB58066 from Abcam to repeat ChIP-seq. It yielded a total of 1061 binding sites that largely overlapped with SC-1703 sites (Figure 1B). Moreover, technical replicates for each antibody also displayed high consistency (Supplementary Figure S1B–F). All the above data demonstrate good quality of our data. Interestingly, only 626 sites were found in MTs (Supplementary Table S2), consistent with the decreased level of YY1 protein in MTs as compared to MBs (Wang *et al*, 2007). No significant overlapping between MB and MT sites was found (Supplementary Figure S1G; Supplementary Table S2), suggesting a drastic change in YY1 binding during differentiation. Among all the binding sites in MBs, 1097 (60.3%) occurred in the promoter region ( $\pm 2$  kb from the transcription start site, TSS) of known RefSeq genes (Figure 1C and D), suggesting a transcriptional regulation on these genes. In all, 248 (13.6%) were found within the gene body of annotated RefSeq genes (Figure 1C, gene body). Strikingly, more than a quarter of these sites (475, 26.1%) occurred in intergenic regions distal from annotated TSSs. In order to validate our ChIP-seq analysis, 15 bound sites were randomly chosen for ChIP-PCR and an enrichment fold ranging from  $\sim 5$  to  $>100$  was obtained for these sites (Figure 1E; Supplementary Table S3). When examining YY1 occupancy at an intermediate differentiating stage (DM 1 day) and fully differentiated MTs (DM 5 day), we found that the binding can be persistently high on some genes but continuously declined on others as differentiation proceeded; on a few genes the occupancy reached the lowest in the intermediate stage. These patterns suggested a dynamic binding of YY1 (Supplementary Figure S1H).

*De novo* prediction of highly enriched DNA sequences from the YY1-binding sites revealed a canonical YY1-bound motif,

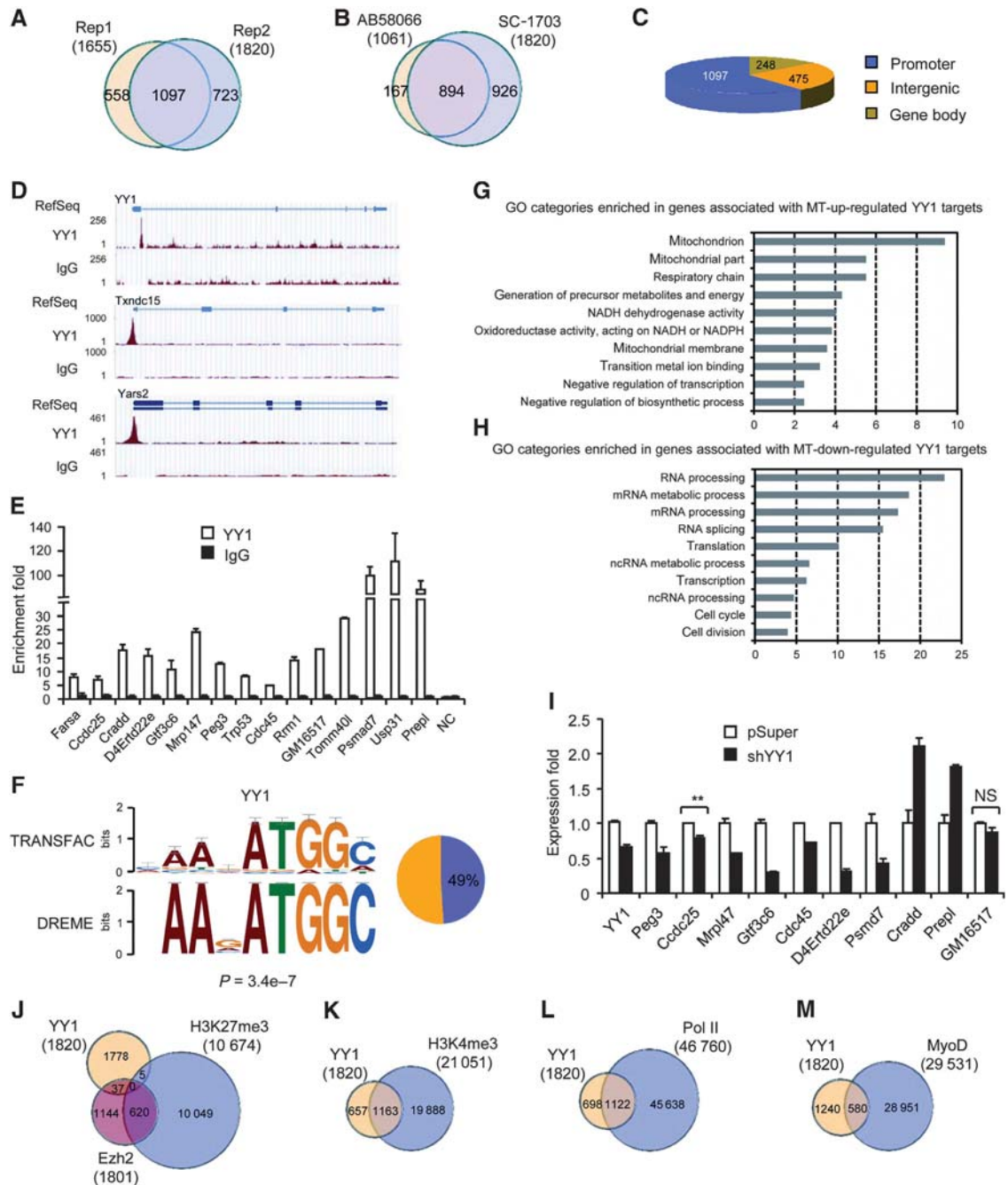


**Figure 1** Genome-wide YY1 occupancy in C2C12 myoblasts. (A) Venn diagrams showing the overlap between identified peaks of two independent biological replicates (rep) of YY1 SC-1703 ChIP-seq. (B) Venn diagrams showing the overlap between identified peaks of YY1 ChIP-seq using two different antibodies AB58066 and SC-1703. (C) Distribution of YY1-binding peaks in C2C12 myoblasts. Promoter = TSS  $\pm$  2 kb. (D) Genomic snapshots depicting the ChIP-seq results for YY1 and IgG at promoter regions of the selected genomic loci. (E) The results of ChIP-PCR validation for 15 selected YY1-binding sites associated with RefSeq gene promoters. Negative control (NC) represents a genomic region without YY1-binding peak identified. (F) *De novo* motif prediction by DREME of DNA sequences enriched in YY1 binding regions. YY1 TRANSFAC matrix is presented for comparison. (G, H) GO analysis of YY1-bound genes that are upregulated or downregulated in MTs compared with MBs. The y axis shows GO terms and the x axis shows statistical significance (i.e., *P*-value) for the top 10 enriched terms. (I) Expression of YY1 target genes in C2C12 cells stably expressing an shYY1 sequence or a vector control, pSuper. (J–M) Venn diagrams showing the overlap between target genes of the indicated ChIP-seq data sets. All PCR data were normalized to GAPDH mRNA and represent the average of three independent experiments  $\pm$  s.d. **\*\****P* < 0.01; NS, not significant.

AAATGGC, among the top 10 scored motifs (49% of the binding sites contain this motif) (Figure 1F), strongly suggesting that YY1 genome-wide association with chromatin is directly mediated by its DNA binding activity.

We next examined the functionality of YY1 binding by looking into the expression of those genes bound by YY1 at

their promoter regions. YY1 is gradually downregulated as C2C12 cells begin to differentiate (Wang *et al*, 2007). If YY1 is required for activation or repression of their target loci, then they should be differentially expressed in MTs versus MBs. To test this hypothesis, we calculated and compared expression of the genes in differentiating MTs versus proliferating MBs using

publicly available RNA-seq data sets (Trapnell *et al*, 2010). A total of 230 YY1-bound genes were found to be upregulated in MTs versus MBs (Supplementary Table S4), suggesting that YY1 may act to repress these genes in MBs. Interestingly, a larger number (472) was found to be highly expressed in MBs but downregulated in MTs, suggesting that YY1 may be necessary for activation of these genes. To gain further insights into the functional relevancy of YY1 binding, we analysed the association of these genes in gene ontology (GO) biological processes. The increased targets were significantly enriched in metabolism-related processes, such as mitochondrion, respiratory chain, and biosynthetic process, suggesting a role of YY1 in regulating mitochondria function and metabolism during skeletal muscle differentiation (Figure 1G; Supplementary Table S4). The decreased targets, on the other hand, were enriched for RNA-related processes and cell cycle/division (Figure 1H; Supplementary Table S4). Experimentally, YY1 knockdown in C2C12 cells by stably expressing a YY1-specific shRNA targeting sequence led to downregulation of eight genes randomly selected from the MT-decreased list and upregulation of two genes from the MT-increased list (Figure 1I), in agreement with dual regulatory roles of YY1.

Others' and our previous work demonstrated that YY1 functions to recruit PRC2 on several muscle structural genes and muscle relevant miRNA loci (Caretti *et al*, 2004; Wang *et al*, 2007, 2008). We asked whether YY1 recruiting PRC2 is a genome-wide event. To test this notion, Ezh2 and H3K27me3 ChIP-seq were performed in C2C12 cells (Supplementary Table S1). A total of 1801 Ezh2-binding sites were identified in MBs (Supplementary Table S5). Surprisingly, only a very small number (2.0%) overlapped with YY1 binding (Figure 1J; Supplementary Table S6). Similarly, a very few H3K27me3 regions overlapped with YY1 despite a significant overlapping between Ezh2 and H3K27me3 binding sites (34.4%, Figure 1J; Supplementary Table S6). The same findings were made when publicly available Ezh2 and H3K27me3 ChIP-seq data sets (Asp *et al*, 2011; Mousavi *et al*, 2012) were used for the analyses (Supplementary Table S6). In addition, the distribution of Ezh2-binding sites was drastically different from YY1 with a large fraction (42.8%) occurred in gene bodies (Supplementary Figure S2A). Furthermore, GO analysis of differentially expressed Ezh2 target genes revealed an enrichment of GO terms drastically different from YY1 (Supplementary Table S7). MT-increased Ezh2-bound genes were enriched for 'Nucleotide binding', 'Protein kinase activity', etc.; and MT-decreased Ezh2-bound genes were enriched for 'Actin binding', 'Actin cytoskeleton', etc. Conversely, YY1 sites strongly overlapped (63.9%) with H3K4me3 regions from our ChIP-seq analysis (Figure 1K; Supplementary Table S6), suggesting that YY1 is associated with actively transcribed promoters defined by H3K4me3. This was further strengthened by a significant overlapping between YY1 and publicly available Pol II binding regions (Asp *et al*, 2011) (Figure 1L; Supplementary Table S6).

To test the potential interplay between YY1 and muscle master regulator, we compared YY1 and publicly available MyoD ChIP-seq data sets (Cao *et al*, 2010). Interestingly, a significant co-occupancy of YY1 with MyoD-binding sites (31.9%) was observed in C2C12 MBs (Figure 1M; Supplementary Table S6). This is in contrast to our previous finding that YY1 and MyoD are exclusive on some muscle loci (Wang *et al*, 2007).

### **YY1 is associated with lincRNA loci and *Yam-1* is positively regulated by YY1**

The significant overrepresentation of ncRNA-related GO terms (e.g., ncRNA processing and ncRNA metabolic process) prompted us to think that YY1 is somehow related to ncRNA regulation. Indeed, among 1097 binding sites localized in a promoter region, 5.4% (59) were associated with known ncRNAs annotated by RefSeq (Figure 2A). Furthermore, considering a large portion of YY1 binding was detected in intergenic regions, we speculated that YY1 might be associated with lincRNA loci and regulate their expression. To test this notion, we examined 475 intergenic binding sites closely and found out that a significant portion (13.3%) was within 100 kb of these novel lincRNAs loci originally identified by Guttman *et al* (2009) (Figure 2B; Supplementary Table S8), suggesting a possible regulation of these lincRNAs by YY1. Subsequent ChIP-PCR on four selected lincRNAs validated our findings by ChIP-seq. Indeed, an enrichment of YY1 was found upstream of these lincRNAs in MBs but not in MTs (Figure 2C). We named these lincRNAs YY1-associated muscle lincRNAs or Yams. Among them, *Yam-1* is located on chromosome 17 with a strong enrichment of YY1 687 bp upstream (Figure 2D, red track). In addition, this lincRNA is highly expressed in C2C12 cells by PolyA + RNA-seq analysis (Figure 2D, blue track), and is characterized with a classical 'K4-K36' histone domain and Pol II binding that define an actively transcribed region (Figure 2D, green tracks).

To test whether the association of YY1 on a *Yam-1* promoter region exerts any functional regulation, we first examined its expression levels in C2C12 MBs with YY1 ectopically overexpressed or knocked down by siRNA oligos (siYY1). Indeed, overexpression of YY1 increased its expression whereas downregulation of YY1 decreased its expression (Figure 2E), suggesting that YY1 positively regulates *Yam-1* in C2C12 MBs. In line with these results, knockdown of YY1 in freshly isolated primary MBs (PMs) also decreased their expression (Figure 2F). Lastly, to test if this regulation occurs *in vivo*, we employed a widely used muscle regeneration model in which injection of CTX results in muscle injury and in turn induces muscle regeneration (Lu *et al*, 2012). Our results showed that injection of siYY1 oligos into CTX-induced regenerating muscles downregulated *Yam-1* expression at multiple time points during the regeneration (Figure 2G). Collectively, these results support a positive regulation of YY1 on *Yam-1* both in cultured muscle cells *in vitro* and in muscle regeneration *in vivo*.

### ***Yam-1* functions as an inhibitor of myogenesis**

The regulation of YY1 on *Yam-1* suggested that *Yam-1* may be a functional lincRNA during myogenesis. From *de novo* assembly of the RNA-seq reads by Cufflinks, it appeared as a PolyA + single exonic transcript. Indeed, rapid amplification of cDNA Ends (RACEs) led to identification of a 923-nt transcript, which is generated from the minus strand (Figure 3A; Supplementary Figure S3). RNA-fluorescence *in situ* hybridization (RNA-FISH) detection revealed that it resides both in nuclei and in cytoplasm of C2C12 MBs in contrast to exclusive nuclear location of U1, a known small nuclear RNA (Figure 3B). This is confirmed by cellular fractionation assay. Nearly equal amount of *Yam-1* was detected in both nuclear and cytoplasmic portions of

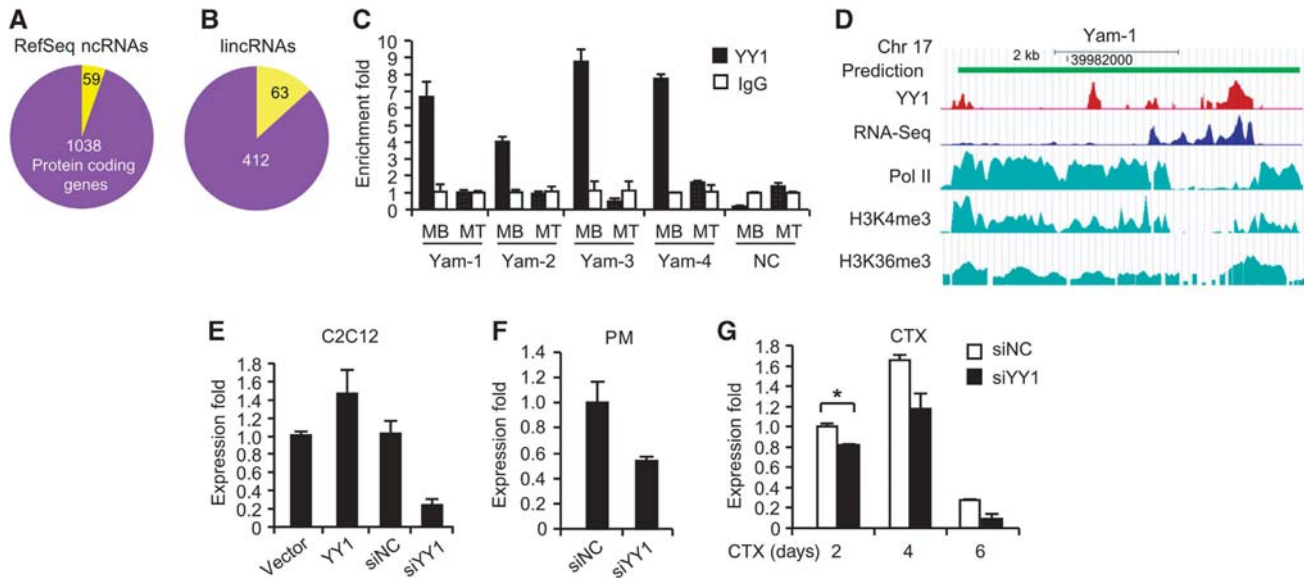


**Figure 2** YY1 is associated with lincRNA loci and positively regulates *Yam-1*. (A) The number of known RefSeq ncRNAs associated with YY1-bound promoter peaks. (B) The number of novel lincRNAs associated with YY1-bound intergenic peaks. (C) ChIP-PCR validation of YY1 binding on *Yam-1-4*. Negative control (NC) represents a genomic region without YY1-bound peak detected in ChIP-seq. (D) Genomic snapshots of *Yam-1* generated in YY1 (red track), Pol II, H3K4me3, H3K36me3 ChIP-seq (green tracks), and RNA-seq (blue track). (E) C2C12 myoblasts were transfected with YY1 expressing plasmid using empty vector as a control or siYY1 oligos using siNC as a control. The expression of *Yam-1* was measured at 48 h post transfection. (F) Primary myoblasts (PMs) were transfected with siNC or siYY1 oligos. The expression level of *Yam-1* was measured at 48 h post transfection. (G) siNC and siYY1 oligos were injected into Cardiotoxin-injured muscles on left and right legs, respectively. The expression of *Yam-1* was detected at the indicated days post injection.  $N = 6$  mice for each group. All PCR data were normalized to GAPDH mRNA and represent the average of three independent experiments  $\pm$  s.d.  $*P < 0.05$ .

C2C12, while U1 and a well-known nuclear lincRNA, Xist, were found highly enriched in nuclear portion (Figure 3C). To test its functionality, we first examined its expression profile during C2C12 differentiation. An increased expression was observed as C2C12 MBs proliferated from  $\sim 30\%$  ( $-1$  day, 1 day prior to transition to differentiation medium, DM) to  $\sim 80\%$  confluence (DM 0 day), but it gradually decreased during the course of myogenic differentiation (Figure 3D). This pattern was also observed during myogenic differentiation of freshly isolated mouse PMs (Figure 3E), suggesting that *Yam-1* may act to inhibit myogenic differentiation. In addition, its expression was rapidly induced by CTX injection, but sharply declined during the regeneration phase starting around day 2 (Figure 3F). Moreover, high expression levels of *Yam-1* were observed in limb muscles of young mice, which displayed active myogenesis but decreased as the perinatal myogenesis ceased after 2 weeks; it remained low as mice grew older (Figure 3G), suggesting that *Yam-1* is associated with active myogenesis *in vivo*.

To investigate if *Yam-1* indeed represses C2C12 myogenic differentiation, it was knocked down in C2C12 MBs by siRNA oligos (si*Yam-1*). A continuous decrease in *Yam-1* during a 2-day period of differentiation led to a marked increase in three myogenic markers, *Myogenin*, *Tnni2*, and  $\alpha$ -*Actin*, at mRNA levels (Figure 3H; Supplementary Figure S4A). Additional evidence came from increased number of MT formation and Troponin positively stained cells (Figure 3I and J) as well as upregulated Troponin protein (Figure 3K) upon si*Yam-1* treatment. Lastly, si*Yam-1* increased the activities of all three muscle genes, *Myogenin*, *Tnni*, and *MyHC* luciferase reporters in differentiating C2C12 MTs (Figure 3L; Supplementary Figure S4B). Together, these results suggest that *Yam-1* functions to suppress myogenic differentiation

of C2C12 cells, which phenocopies the previously known anti-myogenic function of YY1 (Wang *et al*, 2007). Indeed, knockdown of *Yam-1* rescued the inhibitory effect of YY1 on C2C12 differentiation (Figure 3M), confirming that YY1 is functionally upstream of *Yam-1*.

#### Knockdown of *Yam-1* accelerates injury-induced muscle regeneration *in vivo*

To extend our *in vitro* findings to *in vivo* muscle formation, we explored the function of *Yam-1* in CTX-induced muscle regeneration model. siNC or si*Yam-1* oligos were injected into CTX-injured TA muscles following the administration scheme outlined in Figure 4A. Six hours after CTX injection into TA muscles, siNC or si*Yam-1* oligos were administered into left and right hind limbs, respectively. The injections were made every 2 days for a total of three times. The treated muscles were collected at days 1, 2, 3, and 6. Results from qRT-PCR analyses revealed that the expression of *Yam-1* was decreased at all three time points (Figure 4B), suggesting a successful knockdown of *Yam-1* by this approach. Expression levels of MyoD, Myogenin, and embryonic MyHC (eMyHC, a marker for regenerating fibres) were found upregulated by si*Yam-1* injection (Figure 4B), suggesting an acceleration of myogenic program as discovered *in vitro*. Consistently, IF staining on the muscle sections revealed an increased number of Myogenin and eMyHC-positive cells with si*Yam-1* injection (Figure 4C and D). H&E staining showed accelerated regeneration morphology as higher number of newly formed fibres with centrally localized nuclei (CLN) were observed on si*Yam-1*-injected muscles (Figure 4E). This is in keeping with the accelerated regeneration with siYY1 oligo injection (Figure 4E), further demonstrating the positive regulation of *Yam-1* by YY1. Consistently, knockdown of *Yam-1* rescued

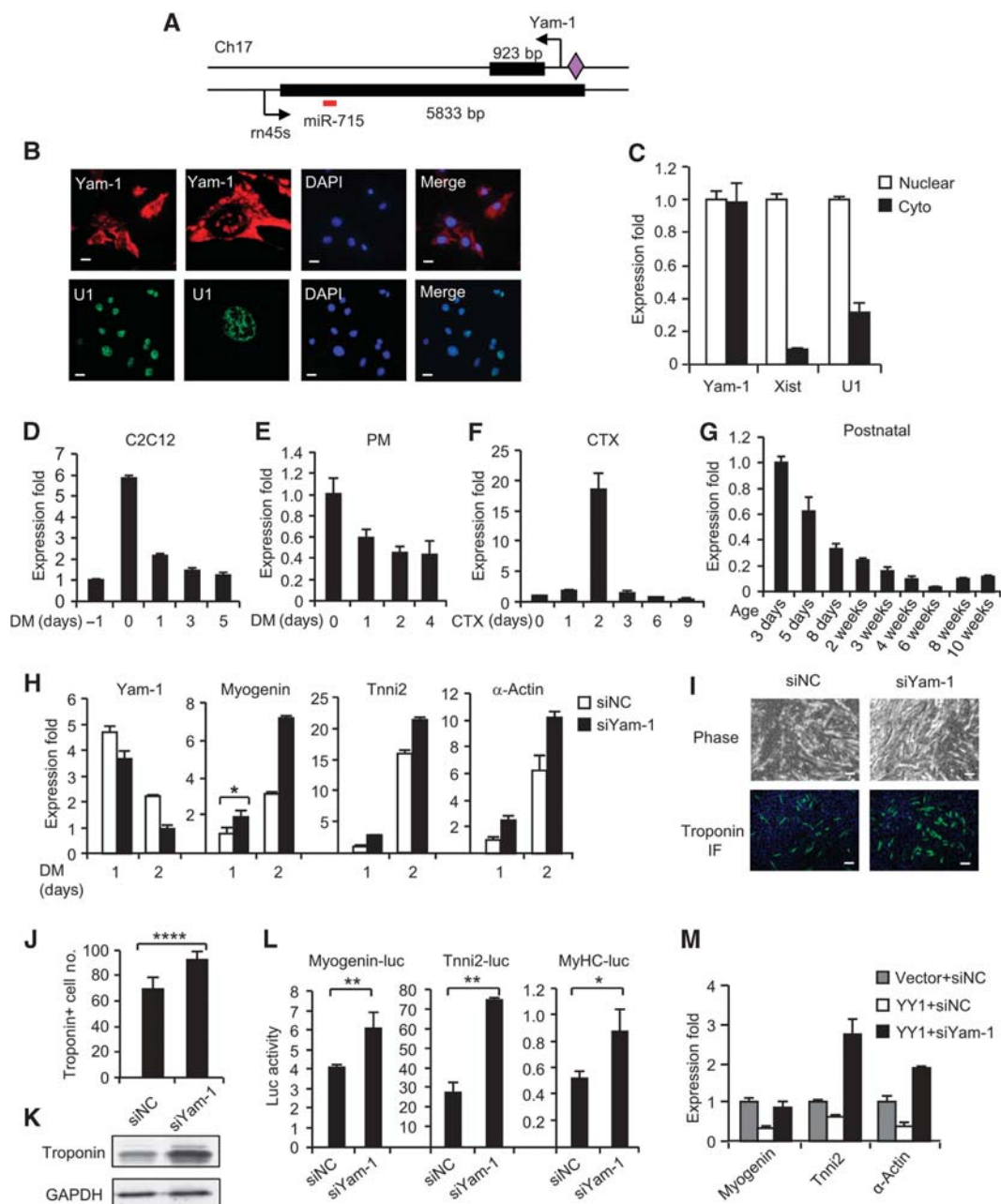


**Figure 3** *Yam-1* inhibits skeletal muscle differentiation. (A) Schematic illustration of *Yam-1* genomic locus on chromosome 17. One of the identified YY1-binding sites is shown as a purple diamond. miR-715 is located ~3 kb downstream and possibly derives from Rn45 transcript, which overlaps with *Yam-1* on the antisense direction. Arrows denote TSS. (B) RNA-FISH was performed on fixed C2C12 myoblasts to visualize the localization of *Yam-1*. DAPI was used to stain the nuclei. Staining of nuclear RNA U1 was used as a positive control. Scale bar = 20  $\mu$ m. (C) The expression of *Yam-1*, Xist, and U1 in nuclear or cytoplasmic fraction of C2C12 myoblasts. (D) The expression of *Yam-1* in differentiating C2C12. -1 day represents proliferating myoblasts at a confluence of 30%. 0 day represents myoblasts at 80% confluence when transferred into DM. (E) The expression of *Yam-1* in differentiating primary myoblasts. (F) The expression of *Yam-1* during CTX-induced regeneration. (G) The expression of *Yam-1* in muscles of postnatal mice at the indicated ages. (H) C2C12 myoblasts were transfected with siYam-1 or siNC oligos. Cells were differentiated for the indicated days and measured for the expression of *Yam-1*, *Myogenin*, *Tnni2*, or  $\alpha$ -Actin RNAs. (I) The above-transfected cells were visualized by phase-contrast microscopy and immunostained for Troponin. Scale bar = 50  $\mu$ m. (J) Positively stained cells were counted from a minimum of 10 randomly chosen fields from 3 individual plates. (K) Troponin protein was probed by western blotting using GAPDH as a loading control. (L) C2C12 cells were transfected with siNC or siYam-1 oligos together with the indicated reporter plasmids. Cells were differentiated for 2 days at 24 h post transfection at which time luciferase activities were determined. The data were normalized to Renilla protein and represent the average of three independent experiments  $\pm$  s.d. (M) C2C12 cells were transfected with the indicated combination of plasmid and siRNA oligos. Cells were switched to DM at 24 h post transfection. The degree of differentiation was assessed after 48 h by measuring the expression of three myogenic markers. All PCR data were normalized to GAPDH mRNA and represent the average of three independent experiments  $\pm$  s.d. \* $P$ <0.05, \*\* $P$ <0.01, \*\*\*\* $P$ <0.0001.

the inhibitory effect of YY1 overexpression on muscle regeneration (Supplementary Figure S4C), whereas overexpression of *Yam-1* suppressed the pro-myogenic effect of siYY1 injection

(Supplementary Figure S4D). Interestingly, the number of proliferating Pax7-positive satellite cells was found to be decreased by siYam-1 injection (Figure 4E), which is likely a

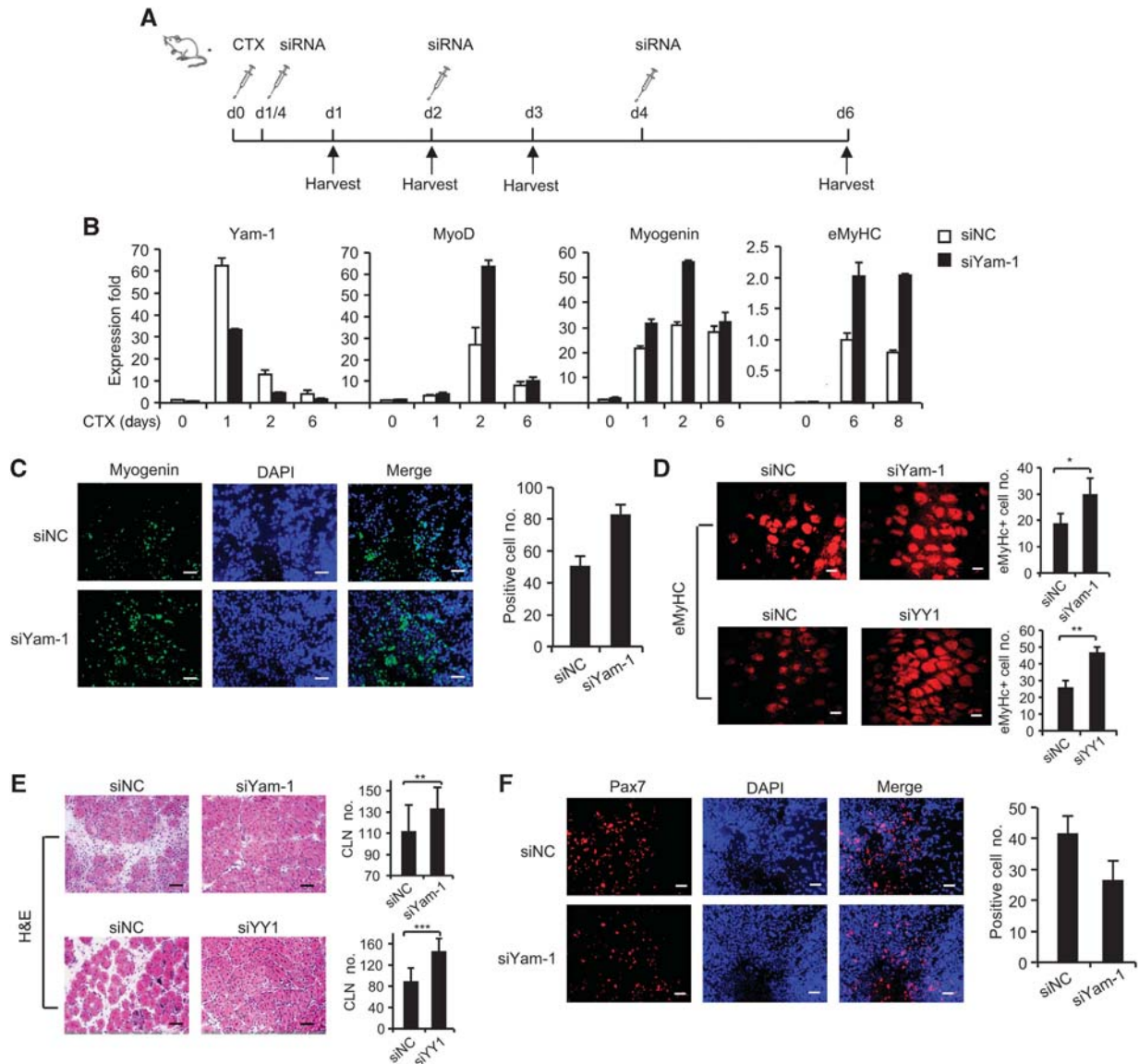


**Figure 4** Knockdown of *Yam-1* improves muscle regeneration *in vivo*. (A) Injection scheme for siNC or siYam-1 into CTX-injured muscles.  $N=4$  mice for each group. (B) The expression of *Yam-1* and myogenic markers in the above-injected muscles. The data were normalized to GAPDH mRNA and represent the average of three independent experiments  $\pm$  s.d. (C) IF staining for Myogenin was performed on the above-injected muscles at day 3. Scale bar = 50  $\mu$ m. The positively stained cells were quantified. (D) siYam-1 or siYY1 oligos were injected into CTX-injured muscles with siNC as controls. The above fibres were stained for eMyHC. Scale bar = 50  $\mu$ m. The positively stained fibres were quantified. (E) The muscles were stained with H&E at day 6. Scale bar = 100  $\mu$ m. Fibres with centrally localized nuclei (CLN) were quantified. (F) IF staining for Pax7 was performed on muscles. Scale bar = 50  $\mu$ m. All the quantification was performed on a minimum of 10 images. \* $P<0.05$ , \*\* $P<0.01$ , and \*\*\* $P<0.001$ .

consequence of accelerated differentiation. Together, these findings imply that *Yam-1* is a functional anti-myogenic factor during muscle regeneration *in vivo*.

#### A YY1-*Yam-1*-miR-715 regulatory axis in myogenesis

To probe into the mechanisms through which *Yam-1* may repress myogenesis, we found an miRNA, miR-715, ~3 kb downstream of *Yam-1* (Figure 3A). Knowing that *in cis* regulation on neighbouring genes is a popular mechanism for lincRNAs action, we tested whether *Yam-1* regulates miR-715 in muscle cells. The expression profiles of miR-715 during C2C12 or PM differentiation mirrored that of *Yam-1* showing a gradual decrease (Figure 5A and B). Its expression was also dynamically regulated in the course of CTX-induced muscle

regeneration with a peak at day 3, 1 day later than *Yam-1*, suggesting a possible induction of miR-715 by *Yam-1* (Figure 5C). Indeed, knockdown of *Yam-1* by siRNA oligos (siYam-1) in C2C12 MBs decreased the expression of miR-715 (Figure 5D), further supporting a positive interplay between them. Interestingly, when further examining other neighbouring genes, we found that siYam-1 treatment led to a significant decrease in five nearby genes (Zfp57, Gabbr1, Cenpq, Mut, and Cd2ap), but to a less degree than its inhibition on miR-715 (Supplementary Figure S5A). Moreover, overexpression of YY1 increased miR-715, while knockdown of YY1 decreased its expression (Figure 5E), suggesting the existence of a YY1-*Yam-1*-miR-715 regulatory axis in C2C12. Also, knockdown of YY1 in the CTX-induced

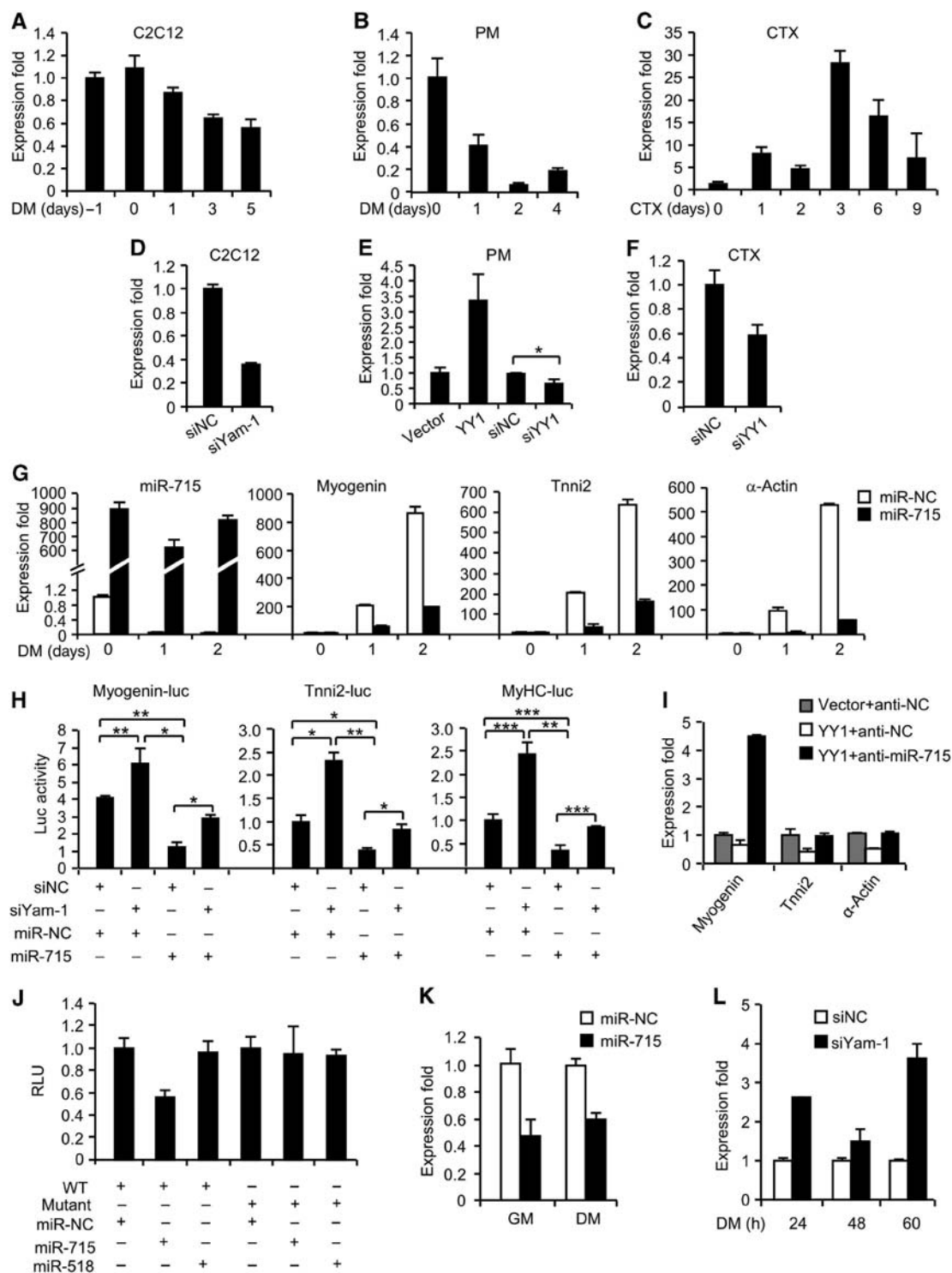


**Figure 5** Functional regulation of miR-715 expression by *Yam-1* during C2C12 myogenesis. (A) The expression of miR-715 was measured in differentiating C2C12; (B) differentiating primary myoblasts, or (C) CTX-injected muscles. (D) C2C12 myoblasts were transfected with siNC or siYam-1 oligos. The expression of miR-715 was measured at 2 days post transfection. (E) PMs were transfected with the indicated expression plasmid or siRNA oligos. The expression of miR-715 was measured at 48 h post transfection. (F) The expression of miR-715 in CTX-induced muscles. (G) C2C12 cells were transfected with miR-715 or negative control (NC) miRNA oligos. Cells were then differentiated (DM) for the indicated days, at which time the expression of miR-715 or the myogenic markers was measured. (H) C2C12 cells were transfected with the indicated reporter plasmids together with a combination of the indicated siRNA and miRNA oligos, and differentiated for 2 days at which time the reporter activities were determined. (I) C2C12 cells were transfected with the indicated combination of plasmid and anti-miRNA (anti) oligos. The degree of differentiation was assessed by measuring the expression of three myogenic markers. (J) A wild-type (WT) or mutant Wnt7b 3'UTR luciferase reporter was transfected into C2C12 cells with the indicated miRNA oligos. Luciferase activities were determined at 48 h post transfection. (K) Wnt7b mRNA expression was measured in NC- or miR-715-transfected C2C12 cells. (L) Wnt7b mRNA expression was measured in siNC- or siYam-1-transfected C2C12 cells. All PCR data were normalized to GAPDH for mRNAs or U6 for miRNAs and represent the average of three independent experiments  $\pm$  s.d. All luciferase data were normalized to Renilla protein and represent the average of three independent experiments  $\pm$  s.d. \* $P$ <0.05, \*\* $P$ <0.01, and \*\*\* $P$ <0.001.

regenerating muscle downregulated miR-715 (Figure 5F), confirming the presence of this regulation *in vivo*. Lastly, to test the functionality of *Yam-1*-miR-715 regulatory axis during skeletal myogenesis, we found that overexpression of miR-715 inhibited C2C12 differentiation as assessed by marked downregulation of Myogenin, Tnni2, and  $\alpha$ -Actin mRNAs (Figure 5G). This is consistent with the anti-myogenic action of *Yam-1*. Furthermore, we found that overexpression of miR-715 attenuated the pro-myogenic effect of si*Yam-1* treatment as assessed by reporter assays using the Myogenin, Tnni2, and MyHC luciferase reporters (Figure 5H). Both *in vitro* and *in vivo*, knockdown of miR-715 rescued the anti-myogenic effect of YY1 overexpression (Figure 5I; Supplementary Figure S5B and C). Altogether, these results indicate that miR-715 is a downstream effector of YY1-*Yam-1* during myogenesis. To further probe into targets of miR-715, we found that Wnt7b is one of the predicted targets with a binding site on its 3' UTR region (Supplementary Figure S5D). Wnt signalling is thought to promote the differentiation of satellite cells and MBs (von Maltzahn *et al*, 2012). To test whether the predicted site mediates Wnt7b targeting by miR-715, a reporter plasmid was generated by cloning this site into pMIR-reporter vector. Co-transfection of the resultant reporter plasmid with miR-715 oligos led to ~40% repression on luciferase activity (Figure 5J). On the contrary, co-transfection of NC oligos or an irrelevant miR-518 oligos did not show such repression. Furthermore, when the putative binding site was mutated, the repression on reporter activity was abolished (Figure 5J, mutant). At the functional level, we predicted that miR-715 binding to the Wnt7b 3'UTR would lead to repression of Wnt7b level. Consistent with this prediction, transfection of the miR-715 oligos caused a decrease in Wnt7b mRNA (Figure 5K). Additionally, *Yam-1* knockdown led to upregulation of Wnt7b expression (Figure 5L), suggesting the existence of *Yam-1* regulation on Wnt7b possibly through miR-715.

### ***Yam-2* promotes early myogenic differentiation**

To better illustrate the functional involvement of Yams in myogenesis, we further investigated roles of *Yam-2*, *Yam-3*, and *Yam-4*. *Yam-2*, a likely single-exonic transcript on mouse chromosome 3 (Supplementary Figure S6A), is also found to be positively regulated by YY1 both in MB cells and in muscle regeneration (Supplementary Figure S6B–D). Unlike *Yam-1*, *Yam-2* was lowly expressed in MBs and significantly induced in the early differentiating stage of both C2C12 myoblast and PMs (Figure 6A and B). *In vivo*, in both CTX-induced muscle regeneration (Figure 6C) and postnatal muscles (Figure 6D), similarly to *Yam-1*, the expression of *Yam-2* was tightly regulated, suggesting its relevancy to muscle development. The early rise of *Yam-2* in C2C12 myogenic differentiation suggested to us that it might be a pro-myogenic factor during the initial stage of differentiation. Indeed, knockdown of *Yam-2* by siRNA oligos (si*Yam-2*) delayed the myogenic program as assessed by decreased expression levels of Myogenin, Tnni2, and  $\alpha$ -Actin mRNAs (Figure 6E) as well as reduced numbers of MT formation, Troponin positively stained cells, and upregulated Troponin protein (Figure 6F–H). Additionally, the activities of Myogenin, Tnni, and MyHC reporters were inhibited in si*Yam-2*-treated cells as compared to negative control (siNC) cells (Figure 6I).

Together, these results suggest that *Yam-2* functions to enhance early myogenic differentiation.

To further strengthen the functionality of Yams, we examined *Yam-3* and *Yam-4* that are located on mouse chromosomes 15 and 6 and regulated by YY1 (Supplementary Figure S6E–H). Consistent with their distinct expression patterns (Supplementary Figure S6I and J), siRNA knockdown of *Yam-3* accelerated C2C12 differentiation, while knockdown of *Yam-4* led to the opposite (Figure 6J and K). Altogether, these findings show that YY regulated Yams exert diverse functions in skeletal myogenesis.

Lastly, to find out whether Yams are evolutionally conserved, we searched for their human orthologues. A transcript of 93.7% homologous with *Yam-1* was found from human chromosome 16 (Supplementary Figure S7A). RNA-seq data available through ENCODE indicated that the human *YAM-1* is highly expressed in several human cell lines. Similarly, potential orthologue of *Yam-3* was also found in human chromosome 22 with a high conservation (88.9%), and evidence of expression was discovered (Supplementary Figure S7B). In contrast, no such human orthologues were found for *Yam-2* and *Yam-4*.

## **Discussion**

By employing high-throughput ChIP-seq combined with computational analyses and experimental validation, our study is the first to identify YY1-binding sites genome-wide in skeletal muscle cells. We found that YY1 is associated with dozens of lincRNA loci. *Yam-1* represents a novel functional lincRNA that exerts a role during myogenic differentiation. *Yam-1*, under positive regulation by YY1, inhibits myogenic differentiation through *in cis* modulation of miR-715 expression, which in turn targets Wnt7b, thus forming a YY1-*Yam-1*-miR-715-Wnt7b regulatory axis (Figure 7).

A total of 1820 YY1-binding sites were identified in proliferating MBs while only 626 in MTs. Unlike what was found in the case of MyoD (Cao *et al*, 2010), a very few genes constitutively bound by YY1 in both MBs and MTs. This is in agreement with gradually declined level of YY1 proteins during C2C12 differentiation. Detailed analysis of YY1 binding revealed several surprising findings: first, in addition to its previously known function as a muscle gene repressor, we found that YY1 could also directly activate a large number of loci, thus playing dual roles in muscle cells. This is in agreement with its well-known dual-acting nature (Gordon *et al*, 2006; Deng *et al*, 2010). Although it is currently unclear how YY1 activates these loci, it probably involves some cofactors that it interacts with. Despite numerous reports demonstrating its interaction with repressive factors such as PRC2, YY1 is known to cooperate with a variety of transcriptional factors linked with transcriptional activation such as Sp1, c-Myc, CREB, p300, and Gata4 to increase transcription (Gordon *et al*, 2006; de Nigris *et al*, 2010; Deng *et al*, 2010; Gregoire *et al*, 2013). Indeed, our prediction of the potential co-regulators within  $\pm 0.2$  kb of YY1-binding peaks revealed a wide variety of transcriptional factors, which could physically interact with YY1 on target loci (Supplementary Figure S2B; Guo *et al*, 2013). Many of them possess gene activating functions, for example, KLF7, GABPA, and Sp1, it is thus likely that YY1 could function with these factors synergistically to activate the target loci. Further

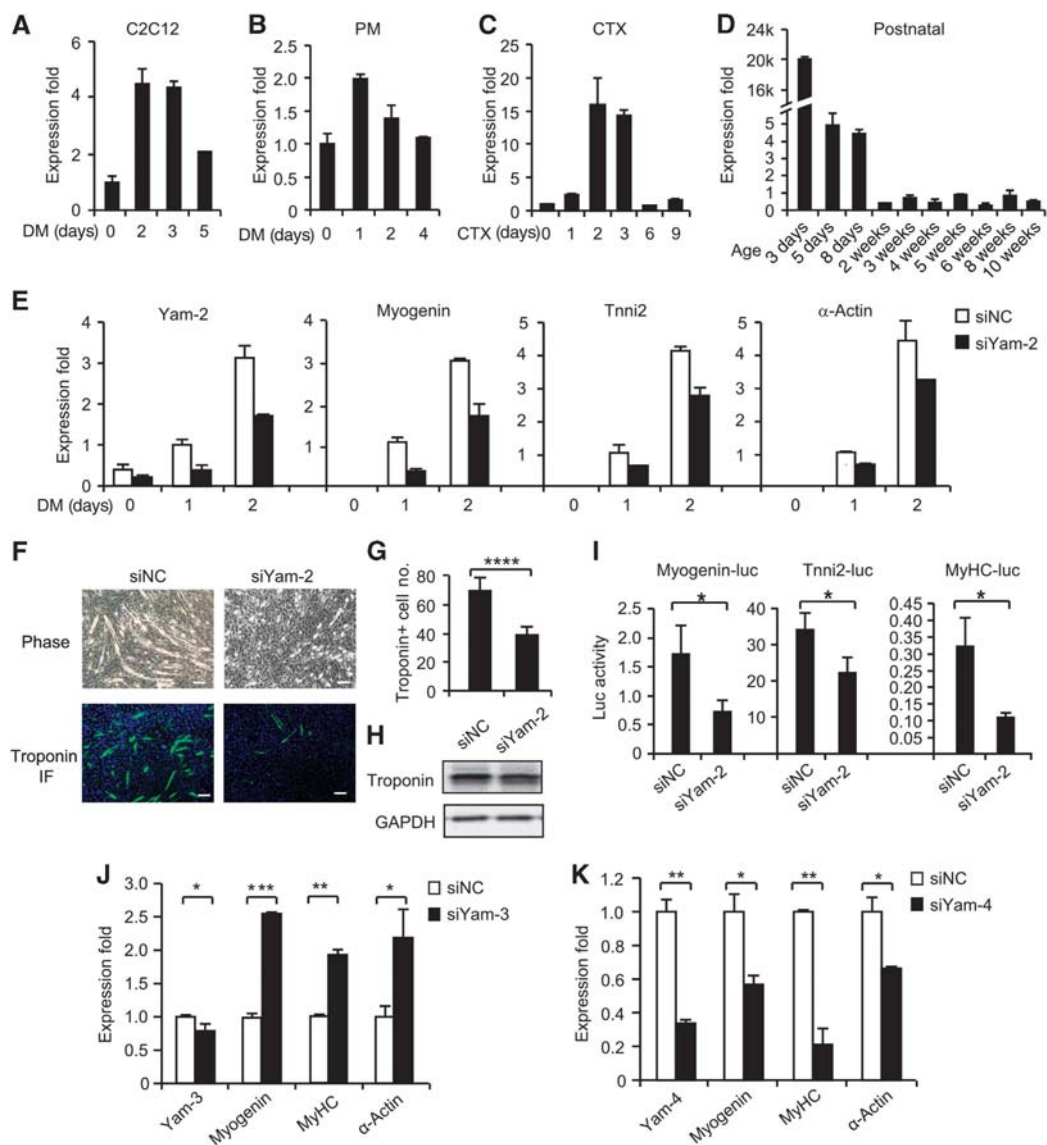


**Figure 6** *Yam-2* promotes early myogenic differentiation. (A) The expression of *Yam-2* in differentiating C2C12; (B) differentiating primary myoblasts; (C) CTX-induced muscle, or (D) postnatal muscles. (E) C2C12 myoblasts were transfected with either si*Yam-2* or siNC oligos. Cells were differentiated for 1 or 2 days at 24 h post transfection. Expression levels of *Yam-2* and myogenic markers were measured. (F) The above-transfected cells were visualized and immunostained for Troponin. Scale bar = 50  $\mu$ m. (G) The positively stained cells were counted from a minimum of 10 randomly chosen fields from 3 individual plates. (H) Troponin protein was probed by western blotting. (I) C2C12 cells were transfected with siNC or si*Yam-2* oligos together with the indicated luciferase reporters. Cells were differentiated at 24 h post transfection for 2 days at which time luciferase activities were determined. The data were normalized to Renilla protein and represent the average of three independent experiments  $\pm$  s.d. (J, K) C2C12 cells were transfected with siRNA oligos against *Yam-3* or *Yam-4*. Cells were differentiated at 24 h post transfection for 2 days at which time the degree of differentiation was assessed by measuring the expression of three markers. All PCR data were normalized to GAPDH mRNA and represent the average of three independent experiments  $\pm$  s.d. \* $P$ <0.05, \*\* $P$ <0.01, \*\*\* $P$ <0.001 and \*\*\*\* $P$ <0.0001.

exploration in the future will be needed to shed lights on this aspect. In all, 472 YY1-bound genes were downregulated in MTs versus MBs while 230 upregulated. We extrapolate to speculate that YY1 is more often an activator than a repressor in MBs. Notably, the genes activated by YY1 are enriched for RNA processing, splicing, and binding, indicating novel roles of YY1 in RNA biology. This is nicely supported by a very recent report demonstrating that YY1 regulates the expression of small non-coding RNAs (sncRNAs) globally in ES cells (Vella *et al*, 2012). Interestingly, our study did not reveal a significant enrichment of YY1 on muscle genes as previously known. Instead, YY1 seems to exert its repressive role mostly on genes related to mitochondrion function and metabolism.

Several studies have associated YY1 with mitochondria biogenesis and oxidative respiration (Calvo *et al*, 2006; Cunningham *et al*, 2007; Xi *et al*, 2007). In particular, Cunningham *et al* (2007) showed that in MTs YY1 binds directly to mitochondrial gene promoters together with PGC-1 $\alpha$  to activate their expression in an mTOR-dependent manner; thus, it is critical for the induction of mitochondrial function and to ensure energy supply. Our findings indicate that YY1 could also silence mitochondrial function in proliferating MBs to ensure a tight control over oxidative metabolism.

Second, it is uncovered that YY1 exerts its function largely independent of PcG despite their co-action on several loci identified before (Wang *et al*, 2007, 2008; Lu *et al*, 2012). This

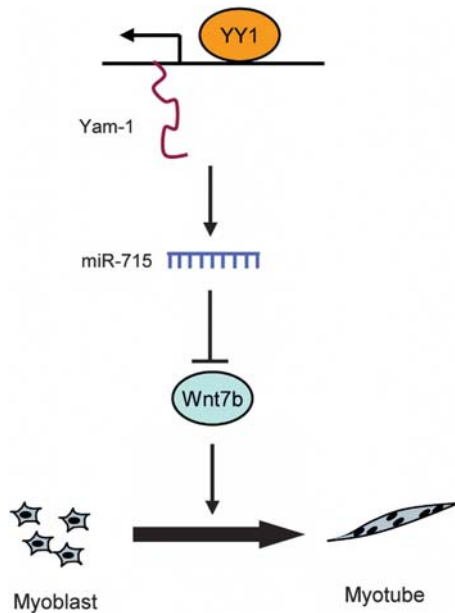


**Figure 7** A model of *Yam-1* in skeletal myogenesis. The model depicts the role of YY1-*Yam-1* axis during myoblasts differentiation into myotubes. YY1 association with *Yam-1* locus modulates its transcription in the myoblasts. *Yam-1* functions to inhibit myoblasts differentiation through regulating the expression of miR-715, which in turn targets *Wnt7b*.

is supported by a recent report in ES cells demonstrating very insignificant co-occupancy between YY1 and PcG bindings (Mendenhall *et al*, 2010; Vella *et al*, 2012). It indicates that YY1 recruiting PcG is probably restricted to very few loci, which is consistent with its predominant role as gene activating not repressing. Indeed, emerging studies are uncovering alternative mechanisms for PcG recruitment to target loci. For example, many lincRNAs are found to be critical for guiding PcG (Brockdorff, 2013). It also suggests that it is important to clarify the real transcriptional nature of a TF at genome-wide level which cannot be achieved by single gene studies. Interestingly, a large portion of YY1 binding overlapped with MyoD. Future elucidation on this aspect will bring novel insights for understanding the function of MyoD and YY1 as well as their interplay.

The most noteworthy finding of this study is to reveal a very novel facet of YY1 regulation, that is, in addition to regulating protein-coding genes, it also controls lincRNA expression. Despite the fast evolving lincRNA field, the evidence of existence and functional characterization of lincRNAs in skeletal myogenesis have barely been explored. Our study not only elucidates the functionality of *Yam-1* in muscle cells, but also its interplay with YY1, demonstrating that lincRNAs are key components of signalling, transcriptional, and chromatin regulatory networks controlling myogenic differentiation. It is worthy to mention that the lincRNA assembly used in our study is from four mouse cell types (ES cells, embryonic fibroblasts, lung fibroblasts, and neural precursor cells) (Guttman *et al*, 2009) because a complete catalogue of lincRNAs of muscle cells is not available yet. Considering lincRNAs are generally expressed in a cell/tissue-specific manner, many muscle-expressing lincRNAs may be missed out in our analysis. Thus, the number of lincRNAs under YY1 regulation could be much larger than 63.

For many TFs, a significant portion of binding can be found in intergenic regions and often dismissed as non-functional association. Our study leads us to believe that the intergenic binding may implicate association with unknown lincRNA loci; in other words, TF regulating lincRNAs may be a general phenomenon that deserves closer investigation. In fact, in ES cells, it was found that a large number of functional lincRNAs were regulated by at least one of the nine pluripotency-associated TFs, including Oct4, Sox2, Nanog, c-Myc, n-Myc, Klf4, Zfx, Smad, and Tcf3 (Guttman *et al*, 2011), suggesting that lincRNAs are important regulatory components within the ES cell circuitry. In agreement with this view, analysis of MyoD ChIP-seq in C2C12 cells revealed 38.7% binding in intergenic regions (Cao *et al*, 2010), probably reflecting its functional regulation on lincRNAs. In the future, it will be interesting to determine the interplay between other TFs and lincRNAs in order to firmly establish that lincRNAs may be an integrated part of the myogenic regulatory network.

The modes through which lincRNAs carry out their regulatory roles are highly diversified. With emerging evidence support their roles in affecting expression largely *in trans* (Guttman *et al*, 2011), some lincRNAs can act *in cis* regulating their neighbour gene expression. For example, 'enhancer RNAs' serve to activate gene expression *in cis* (De Santa *et al*, 2010; Orom *et al*, 2010). Being ~3 kb away from miR-715, our results demonstrated that *Yam-1* seems to act *in cis* regulating miR-715 expression. However, the precise molecular mechanism is still unknown. miR-715 appears to be derived from Rn45s (45s pre-ribosomal RNA), which overlaps with *Yam-1* but is transcribed from the plus strand. It is possible that *Yam-1* could recruit some TF/chromatin modifier locally to Rn45s promoter to influence its transcription. Although not fully understood, it is believed that antisense transcripts are important determinants of the epigenetic regulation of pre-rRNA synthesis (Biefhoff *et al*, 2011). Indeed, we detected a downregulation of Rn45s with *Yam-1* knockdown and also observed H3K27me3 and H3K36me3 marks in its promoter region (data not shown). It is also possible that *Yam-1* affects Rn45s stability through sense-antisense binding. Both as regulatory ncRNAs, the interplay of lincRNAs and miRNAs was largely unexplored. Several recent reports proposed a sponge mode, in which lincRNAs act as a sponge to absorb off the miRNA, preventing it from binding to its targets (Wang *et al*, 2010; Cesana *et al*, 2011). Notably, Cesana *et al* (2011) recently identified that competing endogenous RNA (ceRNA) lincRNA-MD1 could sponge miR-133 and miR-135 to regulate the expression of MAML1 and MEF2C thus controlling muscle differentiation. Our study, on the other hand, suggests that *Yam-1* acts as an upstream regulator of miR-715 expression instead of a sponge. In the future, it will be interesting to further explore the interacting modes between lincRNAs and miR-715. In addition to *Yam-1*, our study has clearly demonstrated that *Yam-2*, *Yam-3*, and *Yam-4* are also functional during myogenesis with the underlying mechanisms awaiting to be discovered. Together, our findings uncover a novel layer of regulation that integrates TF, lincRNA, and microRNA, highlighting the complexity of regulatory network in myogenic differentiation. With the functional roles of lincRNAs discovered in a rapid pace, such regulatory pathways may be pervasive in various biological settings; and the disruption of such pathways may result in development or progression of many human diseases.

## Materials and methods

### Cell culture

Mouse C2C12 MBs were obtained from ATCC and cultured in growth medium (GM) with DMEM, 10% FBS, 2 mM L-glutamine, 100 U/ml penicillin, and 100 µg of Streptomycin at 37°C in 5% CO<sub>2</sub>, or induced to differentiation by culturing the cells in DM (DMEM without FBS containing 2% horse serum) when 90% confluent. PMs were isolated from ~1-week-old C57BL/6 muscles as previously described (Lu *et al*, 2012; Supplementary Methods). The isolated cells were cultured in F10/DMEM medium (1:1) supplemented with 20% FBS and bFGF. The detailed transfection and infection methods can be found in Supplementary Data.

### Oligonucleotides

Precursor miRNA oligos were obtained from Life Technologies. siRNA oligos against mouse YY1, Yam 1, 2, 3, and 4 were obtained from Ribobio Technologies (Guangzhou, China). AntagomiR-NC and miR-715 were obtained from Ribobio and transfected at a 100-nM final concentration. In all, 50 nM siYY1 oligos or miRNA oligos were used for transient transfections. *Yam-1-4* siRNAs were transfected at a final concentration of 150 nM. The sequences of oligonucleotides used for siRNA knockdown, RT-PCR, and Northern, RACE, and ChIP-PCR are provided in Supplementary Table S9.

### DNA constructs

YY1 expression plasmid, Myogenin, TnI, and MyHC reporter plasmids and pSuper-shYY1-GFP plasmid were described before (Wang *et al*, 2007; Yang *et al*, 2013). For *in vitro* transcription, the full-length Yam-1 was cloned into a pBluescript KS II vector with *Bam*H1 and *Xho*I sites. A full-length Yam-1 expression plasmid was generating by cloning Yma-1 into *Bam*H1 and *Xho*I sites of pcDNA 3.1+. To construct Wnt7b-3'UTR reporter plasmids, a 633-bp fragment encompassing the predicted binding site was cloned into pMIR-report vector (ABI) between *Hind*III and *Sac*I sites. A mutant Wnt7b-3'UTR plasmid was generated by changing the miR-715 binding site from GCACGGA to ATGATTG.

### Rapid amplification of cDNA end

SMARTer RACE cDNA Amplification Kit (Clontech) was used according to the manufacturer's instructions. Briefly, to generate 5' RACE-Ready cDNAs, 1 µg of total RNAs extracted from C2C12 MBs was reverse transcribed using 5'-CDS Primer A, SMARTer IIA oligo, and SMARTScribe Reverse Transcriptase. The subsequent PCR amplification was carried out using a gene-specific reverse primer (RP) designed on the basis of RNA-seq-derived sequence and a Universal Primer Mixture (UPM) from the kit. 3' RACE-Ready cDNAs were obtained by using 3'-CDS Primer A.

### RT-PCR and real-time RT-PCR

Total RNAs from cells were extracted using TRIzol reagent (Life Technologies). Expression of mRNA was determined by real-time RT-PCR as described using GAPDH for normalization. Expression of mature miRNAs was determined with the miRNA-specific Taqman microRNA assay kit (Life Technologies) in a 7900HT system (Life Technologies) using U6 for normalization. All the experiments were designed in triplicates. For fractionation assay, cytoplasmic and nuclear RNAs were extracted from C2C12 MBs as previously described (Supplementary Data).

### RNA fluorescence in situ hybridization

To detect Yam-1 RNA location, RNA-FISH was performed as described before (Sone *et al*, 2007) (Supplementary Data). All samples were imaged with ×40 objective lens. Pictures were captured in Kahlman frame giving an average of two scans using the Olympus microscope FV1000 and the accompanying software FV10-ASW (version 01.07.02.02, Olympus).

### Immunoblotting, immunohistochemistry, and immunostaining

Western blotting was performed as previously described (Wang *et al*, 2007). The following dilutions were used for each antibody: Troponin (Sigma, St Louis, USA, Cat# T6277; 1:1000), GAPDH (Santa Cruz Biotechnology, Santa Cruz, CA, USA, Cat# SC-137179; 1:5000). Immunofluorescence of C2C12 cells was performed using a Troponin monoclonal antibody (Sigma, Cat# T6277) and MyoG

polyclonal antibody (Santa Cruz, Cat# SC-576) at 1:500 dilutions. Immunofluorescence on frozen muscle sections was performed using the following antibodies: Pax7 (Santa Cruz Biotechnology, Cat# SC-576, 1:200), Myogenin (DSHB, 1:100), and eMyHC (Leica, Cat# NCL-MHCd). H&E staining on frozen muscle sections was performed as previously described (Diao *et al*, 2012). The number of central nuclei localized fibres was counted from a minimum of 10 randomly chosen fields, from 4 to 5 sections throughout the length of the muscle in 4–6 per group.

### ChIP assays

ChIP assays were performed as previously described (Lu *et al*, 2012; Zhou *et al*, 2012b). In all, 5 µg of antibodies was used for each  $2 \times 10^7$  cell in one immunoprecipitation. YY1 #1 (Santa Cruz Biotechnology, Cat# SC-1703, rabbit polyclonal), YY1 #2 (Abcam, Cat# AB58066, mouse monoclonal), Ezh2 (Cell Signaling, MA, USA, Cat# AC22), trimethyl-histone H3-K27 (Millipore, Cat# 07-449), trimethyl-histone H3-K4 (Millipore, Cat# 07-473), or normal mouse IgG (Santa Cruz Biotechnology, Cat# SC-2025) was used as a negative control. Immunoprecipitated genomic DNA was re-suspended in 10–15 µl of water. PCRs were performed with 1 µl of immunoprecipitated material as a template and products were analysed by qRT-PCR on a 7900HT system (Life Technologies).

### ChIP sequencing

For library construction, we used a protocol as described before (Diao *et al*, 2012). The purified DNA library products were evaluated using a Bioanalyzer (Agilent) and SYBR qPCR and diluted to 10 nM for sequencing on an Illumina Hi-seq 2000 sequencer (YY1) (pair-end with 50 bp) or an Illumina Genome Analyzer Ix sequencer (Ezh2, H3K27me3, and H3K4me3) (pair-end with 36 bp). Technical replicates were prepared by sequencing the same library twice. More details can be found in Supplementary data. All the sequence data have been deposited in NCBI's Gene Expression Omnibus (GEO, <http://www.ncbi.nlm.nih.gov/geo>) (Edgar *et al*, 2002) and are accessible through GEO Series accession number GSE45875.

### Peak defining

The sequenced reads were mapped to the mouse reference genome (UCSC mm9) using SOAP2 (Li *et al*, 2009). The alignments were performed allowing the maximum of two mismatches and keeping only the uniquely aligned reads. The protein DNA binding peaks (sites) were identified using Model-based Analysis for ChIP-seq (MACS, version 2.0.9) (Zhang *et al*, 2008) with IgG control sample as a background. During the peak calling, a *q*-value (adjusted *P*-value calculated using Benjamini-Hochberg procedure) was set under  $10^{-5}$  for YY1 (Supplementary Table S1, corresponding to an empirical FDR of 3.4%) and  $10^{-2}$  for EZH2 and H3K27me3, respectively. Raw ChIP-seq sequencing reads for transcription factor MyoD were downloaded from NCBI's Sequence Read Archive (SRA; <http://www.ncbi.nlm.nih.gov/sra>) with accession number SRX016191 and SRX016040 for MBs and MTs, respectively. MyoD-binding sites were identified using the same *q*-value cutoff as for Ezh2. The processed ChIP-seq data and identified binding sites in MBs and MTs for Pol II and H3K4me3 were obtained from NCBI's GEO under accession number GSE25308. Each identified peak was associated with the closest RefSeq gene when it falls into the 4 kb ( $\pm 2$  kb) flanking region of the gene's TSS.

### De novo motif discovery and analysis and functional annotation

See Supplementary Data.

### Identification of YY1 bound novel lincRNAs

The list of novel lincRNA identified by K4-K36 domain from four mouse cell types was obtained from Guttman *et al* (2009). YY1-binding sites were searched in the flanking regions (~100 kb on both sides) of these lincRNAs. The resultant list of lincRNAs was considered as YY1-associated lincRNAs.

### Statistical analysis

All quantitative data were obtained as triplicates. Data were shown as means  $\pm$  standard deviation (s.d.). Statistical significance between two groups was determined by Student's *t*-test. \**P*<0.05, \*\**P*<0.01, and \*\*\**P*<0.001.

### Animal studies

C57BL/6 mice were housed in the animal facilities of the Chinese University of Hong Kong under conventional conditions with constant temperature and humidity and fed a standard diet. Animal experimentation was approved by the CUHK Animal Experimentation Ethics Committee (Ref No. 10/027/MIS). Postnatal muscles were obtained from tibialis anterior (TA) muscles of different ages of C57BL/6 mice, and RNAs were extracted for real-time RT-PCR analysis. For injury-induced muscle regeneration studies, ~6-week-old C57BL/6 mice were injected with 60  $\mu$ l of CTX (Latoxan, France) at 10  $\mu$ M into the TA muscles. Injections of siRNA oligos were performed 6 h after CTX injection and re-injected every 2 days for a total of three times. In all, 5  $\mu$ M of siYY1 or 15  $\mu$ M of siYam-1 oligos were prepared by pre-incubating with Lipofectamine 2000 for 15 min and injections were made in a final volume of 60  $\mu$ l in OPTI-EM (Life Technologies). For *in vivo* delivery, the combination of Vector, YY1, or Yam-1 expression plasmids (30  $\mu$ g), siNC or siYam1 (0.9 nmol), antagoNC or antago miR-715 (0.5 nmol) were electroporated into the TA muscles using a BTX ECM 830 generator (mode:LV; pulse length: 20 ms; number of pulses: 8) according to Diao *et al* (2012). Muscles were harvested at designated times, and RNAs were extracted for real-time RT-PCR analysis. Frozen muscle sections were prepared and stained as previously described (Wang *et al*, 2012; Zhou *et al*, 2012b).

### References

Asp P, Blum R, Vethantham V, Parisi F, Micsinai M, Cheng J, Bowman C, Kluger Y, Dynlacht BD (2011) Genome-wide remodeling of the epigenetic landscape during myogenic differentiation. *Proc Natl Acad Sci USA* **108**: E149–E158

Bierhoff H, Schmitz K, Maass F, Ye J, Grummt I (2011) Noncoding transcripts in sense and antisense orientation regulate the epigenetic state of ribosomal RNA genes. *Cold Spring Harb Symp Quant Biol* **75**: 357–364

Blattler SM, Cunningham JT, Verdeguer F, Chim H, Haas W, Liu H, Romanino K, Ruegg MA, Gygi SP, Shi Y, Puigserver P (2012) Yin Yang 1 deficiency in skeletal muscle protects against rapamycin-induced diabetic-like symptoms through activation of insulin/IGF signaling. *Cell Metab* **15**: 505–517

Brockdorff N (2013) Noncoding RNA and Polycomb recruitment. *RNA* **19**: 429–442

Buckingham M (2006) Myogenic progenitor cells and skeletal myogenesis in vertebrates. *Curr Opin Genet Dev* **16**: 525–532

Cabili MN, Trapnell C, Goff L, Koziol M, Tazon-Vega B, Regev A, Rinn JL (2011) Integrative annotation of human large intergenic noncoding RNAs reveals global properties and specific subclasses. *Genes Dev* **25**: 1915–1927

Calvo S, Jain M, Xie X, Sheth SA, Chang B, Goldberger OA, Spinazzola A, Zeviani M, Carr SA, Mootha VK (2006) Systematic identification of human mitochondrial disease genes through integrative genomics. *Nat Genet* **38**: 576–582

Cao Y, Yao Z, Sarkar D, Lawrence M, Sanchez GJ, Parker MH, MacQuarrie KL, Davison J, Morgan MT, Ruzzo WL, Gentleman RC, Tapscott SJ (2010) Genome-wide MyoD binding in skeletal muscle cells: a potential for broad cellular reprogramming. *Dev Cell* **18**: 662–674

Caretto G, Di Padova M, Micales B, Lyons GE, Sartorelli V (2004) The Polycomb Ezh2 methyltransferase regulates muscle gene expression and skeletal muscle differentiation. *Genes Dev* **18**: 2627–2638

Cesana M, Cacchiarelli D, Legnini I, Santini T, Sthandier O, Chinappi M, Tramontano A, Bozzoni I (2011) A long noncoding RNA controls muscle differentiation by functioning as a competing endogenous RNA. *Cell* **147**: 358–369

Cunningham JT, Rodgers JT, Arlow DH, Vazquez F, Mootha VK, Puigserver P (2007) mTOR controls mitochondrial oxidative function through a YY1-PGC-1 $\alpha$  transcriptional complex. *Nature* **450**: 736–740

de Nigris F, Crudele V, Giovane A, Casamassimi A, Giordano A, Garban HJ, Cacciatore F, Pentimalli F, Marquez-Garban DC, Petrillo A, Cito L, Sommese L, Fiore A, Petrillo M, Siani A, Barbieri A, Arra C, Rengo F, Hayashi T, Al-Omran M *et al* (2010)

### Supplementary data

Supplementary data are available at *The EMBO Journal* Online (<http://www.embojournal.org>).

### Acknowledgements

We thank Prof Dennis YM Lo and Prof Rossa WK. Chiu for granting us the access to GAIx and HiSeq sequencer and the generous support from their team throughout the course of this study. The work described in this paper was substantially supported by three General Research Funds (GRF) to HW and HS from the Research Grants Council (RGC) of the Hong Kong Special Administrative Region, China (CUHK476309 and 476310 to HW and 473211 to HS), two CUHK direct grants to HW (2041492 and 2041662) and a CUHK direct grant to HS (2041474), private fund from Department of O&G, CUHK.

*Author contributions:* HW and HS conceived and designed the experiments. LL, XC, LW, YZ, and LZ performed the experiments. KS, LL, and HS analysed the data. HW, HS, LL, and KS wrote the paper, HW, HS, LL, and KS reviewed and edited the manuscript.

### Conflict of interest

The authors declare that they have no conflict of interest.

CXCR4/YY1 inhibition impairs VEGF network and angiogenesis during malignancy. *Proc Natl Acad Sci USA* **107**: 14484–14489

De Santa F, Barozzi I, Mietton F, Ghisletti S, Polletti S, Tusi BK, Muller H, Ragoussis J, Wei CL, Natoli G (2010) A large fraction of extragenic RNA pol II transcription sites overlap enhancers. *PLoS Biol* **8**: e1000384

Deng Z, Cao P, Wan MM, Sui G (2010) Yin Yang 1: a multifaceted protein beyond a transcription factor. *Transcription* **1**: 81–84

Diao Y, Guo X, Li Y, Sun K, Lu L, Jiang L, Fu X, Zhu H, Sun H, Wang H, Wu Z (2012) Pax3/7BP is a Pax7- and Pax3-binding protein that regulates the proliferation of muscle precursor cells by an epigenetic mechanism. *Cell Stem Cell* **11**: 231–241

Edgar R, Domrachev M, Lash AE (2002) Gene Expression Omnibus: NCBI gene expression and hybridization array data repository. *Nucleic Acids Res* **30**: 207–210

Gordon S, Akopyan G, Garban H, Bonavida B (2006) Transcription factor YY1: structure, function, and therapeutic implications in cancer biology. *Oncogene* **25**: 1125–1142

Gregoire S, Karra R, Passer D, Deutsch MA, Krane M, Feistritz R, Sturzu A, Domian I, Saga Y, Wu SM (2013) Essential and unexpected role of Yin Yang 1 to promote mesodermal cardiac differentiation. *Circ Res* **112**: 900–910

Guo AM, Sun K, Su X, Wang H, Sun H (2013) YY1TargetDB: an integral information resource for Yin Yang 1 target loci. *Database (Oxford)* **2013**: bat007

Gupta RA, Shah N, Wang KC, Kim J, Horlings HM, Wong DJ, Tsai MC, Hung T, Argani P, Rinn JL, Wang Y, Brzoska P, Kong B, Li R, West RB, van de Vijver MJ, Sukumar S, Chang HY (2010) Long non-coding RNA HOTAIR reprograms chromatin state to promote cancer metastasis. *Nature* **464**: 1071–1076

Guttman M, Amit I, Garber M, French C, Lin MF, Feldser D, Huarte M, Zuk O, Carey BW, Cassady JP, Cabili MN, Jaenisch R, Mikkelsen TS, Jacks T, Hacohen N, Bernstein BE, Kellis M, Regev A, Rinn JL, Lander ES (2009) Chromatin signature reveals over a thousand highly conserved large non-coding RNAs in mammals. *Nature* **458**: 223–227

Guttman M, Donaghey J, Carey BW, Garber M, Grenier JK, Munson G, Young G, Lucas AB, Ach R, Bruhn L, Yang X, Amit I, Meissner A, Regev A, Rinn JL, Root DE, Lander ES (2011) lincRNAs act in the circuitry controlling pluripotency and differentiation. *Nature* **477**: 295–300

Guttman M, Garber M, Levin JZ, Donaghey J, Robinson J, Adiconis X, Fan L, Koziol MJ, Gnirke A, Nusbaum C, Rinn JL, Lander ES, Regev A (2010) Ab initio reconstruction of cell type-specific transcriptomes in mouse reveals the conserved multi-exonic structure of lincRNAs. *Nat Biotechnol* **28**: 503–510

- Huarte M, Guttman M, Feldser D, Garber M, Koziol MJ, Kenzelmann-Broz D, Khalil AM, Zuk O, Amit I, Rabani M, Attardi LD, Regev A, Lander ES, Jacks T, Rinn JL (2010) A large intergenic noncoding RNA induced by p53 mediates global gene repression in the p53 response. *Cell* **142**: 409–419
- Khalil AM, Guttman M, Huarte M, Garber M, Raj A, Rivea Morales D, Thomas K, Presser A, Bernstein BE, van Oudenaarden A, Regev A, Lander ES, Rinn JL (2009) Many human large intergenic noncoding RNAs associate with chromatin-modifying complexes and affect gene expression. *Proc Natl Acad Sci USA* **106**: 11667–11672
- Landt SG, Marinov GK, Kundaje A, Kheradpour P, Pauli F, Batzoglou S, Bernstein BE, Bickel P, Brown JB, Cayting P, Chen Y, DeSalvo G, Epstein C, Fisher-Aylor KI, Euskirchen G, Gerstein M, Gertz J, Hartemink AJ, Hoffman MM, Iyer VR *et al* (2012) ChIP-seq guidelines and practices of the ENCODE and modENCODE consortia. *Genome Res* **22**: 1813–1831
- Li Q, Brown JB, Huang H, Bickel PJ (2011) Measuring reproducibility of high-throughput experiments. *Annals of Applied Statistics* **5**: 1752–1779
- Li R, Yu C, Li Y, Lam TW, Yiu SM, Kristiansen K, Wang J (2009) SOAP2: an improved ultrafast tool for short read alignment. *Bioinformatics* **25**: 1966–1967
- Loewer S, Cabili MN, Guttman M, Loh YH, Thomas K, Park IH, Garber M, Curran M, Onder T, Agarwal S, Manos PD, Datta S, Lander ES, Schlaeger TM, Daley GQ, Rinn JL (2010) Large intergenic non-coding RNA-RoR modulates reprogramming of human induced pluripotent stem cells. *Nat Genet* **42**: 1113–1117
- Lu L, Zhou L, Chen EZ, Sun K, Jiang P, Wang L, Su X, Sun H, Wang H (2012) A novel YY1-miR-1 regulatory circuit in skeletal myogenesis revealed by genome-wide prediction of YY1-miRNA network. *PLoS One* **7**: e27596
- Mendenhall EM, Koche RP, Truong T, Zhou VW, Issac B, Chi AS, Ku M, Bernstein BE (2010) GC-rich sequence elements recruit PRC2 in mammalian ES cells. *PLoS Genet* **6**: e1001244
- Mousavi K, Zare H, Wang AH, Sartorelli V (2012) Polycomb protein Ezh1 promotes RNA polymerase II elongation. *Mol Cell* **45**: 255–262
- Orom UA, Derrien T, Beringer M, Gumireddy K, Gardini A, Bussotti G, Lai F, Zytznicki M, Notredame C, Huang Q, Guigo R, Shiekhattar R (2010) Long noncoding RNAs with enhancer-like function in human cells. *Cell* **143**: 46–58
- Palacios D, Mozzetta C, Consalvi S, Caretti G, Saccone V, Proserpio V, Marquez VE, Valente S, Mai A, Forcales SV, Sartorelli V, Puri PL (2010) TNF/p38alpha/polycomb signaling to Pax7 locus in satellite cells links inflammation to the epigenetic control of muscle regeneration. *Cell Stem Cell* **7**: 455–469
- Paralkar VR, Weiss MJ (2011) A new 'Linc' between noncoding RNAs and blood development. *Genes Dev* **25**: 2555–2558
- Perdiguerro E, Sousa-Victor P, Ballestar E, Munoz-Canoves P (2009) Epigenetic regulation of myogenesis. *Epigenetics* **4**: 541–550
- Prensner JR, Iyer MK, Balbin OA, Dhanasekaran SM, Cao Q, Brenner JC, Laxman B, Asangani IA, Grasso CS, Kominsky HD, Cao X, Jing X, Wang X, Siddiqui J, Wei JT, Robinson D, Iyer HK, Palanisamy N, Maher CA, Chinnaiyan AM (2011) Transcriptome sequencing across a prostate cancer cohort identifies PCAT-1, an unannotated lincRNA implicated in disease progression. *Nat Biotechnol* **29**: 742–749
- Sabourin LA, Rudnicki MA (2000) The molecular regulation of myogenesis. *Clin Genet* **57**: 16–25
- Sone M, Hayashi T, Tarui H, Agata K, Takeichi M, Nakagawa S (2007) The mRNA-like noncoding RNA Gomafu constitutes a novel nuclear domain in a subset of neurons. *J Cell Sci* **120**: 2498–2506
- Trapnell C, Williams BA, Pertea G, Mortazavi A, Kwan G, van Baren MJ, Salzberg SL, Wold BJ, Pachter L (2010) Transcript assembly and quantification by RNA-Seq reveals unannotated transcripts and isoform switching during cell differentiation. *Nat Biotechnol* **28**: 511–515
- Tsai MC, Manor O, Wan Y, Mosammaparast N, Wang JK, Lan F, Shi Y, Segal E, Chang HY (2010) Long noncoding RNA as modular scaffold of histone modification complexes. *Science* **329**: 689–693
- Ulitsky I, Shkumatava A, Jan CH, Sive H, Bartel DP (2011) Conserved function of lincRNAs in vertebrate embryonic development despite rapid sequence evolution. *Cell* **147**: 1537–1550
- Vella P, Barozzi I, Cuomo A, Bonaldi T, Pasini D (2012) Yin Yang 1 extends the Myc-related transcription factors network in embryonic stem cells. *Nucleic Acids Res* **40**: 3403–3418
- von Maltzahn J, Chang NC, Bentzinger CF, Rudnicki MA (2012) Wnt signaling in myogenesis. *Trends Cell Biol* **22**: 602–609
- Wang H, Garzon R, Sun H, Ladner KJ, Singh R, Dahlman J, Cheng A, Hall BM, Qualman SJ, Chandler DS, Croce CM, Guttridge DC (2008) NF-kappaB-YY1-miR-29 regulatory circuitry in skeletal myogenesis and rhabdomyosarcoma. *Cancer Cell* **14**: 369–381
- Wang H, Hertlein E, Bakkar N, Sun H, Acharyya S, Wang J, Carathers M, Davuluri R, Guttridge DC (2007) NF-kappaB regulation of YY1 inhibits skeletal myogenesis through transcriptional silencing of myofibrillar genes. *Mol Cell Biol* **27**: 4374–4387
- Wang J, Liu X, Wu H, Ni P, Gu Z, Qiao Y, Chen N, Sun F, Fan Q (2010) CREB up-regulates long non-coding RNA, HULC expression through interaction with microRNA-372 in liver cancer. *Nucleic Acids Res* **38**: 5366–5383
- Wang L, Zhou L, Jiang P, Lu L, Chen X, Lan H, Guttridge DC, Sun H, Wang H (2012) Loss of miR-29 in myoblasts contributes to dystrophic muscle pathogenesis. *Mol Ther* **20**: 1222–1233
- Xi H, Yu Y, Fu Y, Foley J, Halees A, Weng Z (2007) Analysis of overrepresented motifs in human core promoters reveals dual regulatory roles of YY1. *Genome Res* **17**: 798–806
- Yang L, Lin C, Rosenfeld MG (2011) A lincRNA switch for embryonic stem cell fate. *Cell Res* **21**: 1646–1648
- Yang Y, Zhou L, Lu L, Wang L, Li X, Jiang P, Chan LK, Zhang T, Yu J, Kwong J, Cheung TH, Chung T, Mak K, Sun H, Wang H (2013) A novel miR-193a-5p-YY1-APC regulatory axis in human endometrioid endometrial adenocarcinoma. *Oncogene* **32**: 3432–3442
- Young RS, Marques AC, Tibbit C, Haerty W, Bassett AR, Liu JL, Ponting CP (2012) Identification and properties of 1,119 candidate lincRNA loci in the *Drosophila melanogaster* genome. *Genome Biol Evol* **4**: 427–442
- Zhang Y, Liu T, Meyer CA, Eeckhoutte J, Johnson DS, Bernstein BE, Nusbaum C, Myers RM, Brown M, Li W, Liu XS (2008) Model-based analysis of ChIP-Seq (MACS). *Genome Biol* **9**: R137
- Zhou L, Wang L, Lu L, Jiang P, Sun H, Wang H (2012a) Inhibition of miR-29 by TGF-beta-Smad3 signaling through dual mechanisms promotes transdifferentiation of mouse myoblasts into myofibroblasts. *PLoS One* **7**: e33766
- Zhou L, Wang L, Lu L, Jiang P, Sun H, Wang H (2012b) A novel target of microRNA-29, Ring1 and YY1-binding protein (Rybp), negatively regulates skeletal myogenesis. *J Biol Chem* **287**: 25255–25265